Femtosecond laser absorption in fused silica: Numerical and experimental investigation

Alexander Q. Wu, Ihtesham H. Chowdhury, and Xianfan Xu*
School of Mechanical Engineering, Purdue University, West Lafayette, Indiana 47907, USA
(Received 27 January 2005; revised manuscript received 25 April 2005; published 22 August 2005)

Single pulse transmissivity and reflectivity of fused silica irradiated by tightly focused 90 fs laser pulses at a center wavelength of 800 nm are numerically and experimentally investigated to study the role of nonlinear photoionization and avalanche ionization processes in free electron generation. The laser beam inside fused silica is modeled with a (2+1)-dimensional propagation equation which considers the effects of laser beam diffraction, group velocity dispersion, self-focusing, defocusing, and absorption due to the free electrons and nonlinear photoionization of the valence electrons. Comparison of our simulation to the experimental data reveals that the avalanche ionization coefficients are much smaller than some previously reported results and that avalanche ionization is of minor importance in generating free electrons in fused silica at the laser fluence levels considered in this study.

DOI: 10.1103/PhysRevB.72.085128 PACS number(s): 78.47.+p, 42.65.Re

I. INTRODUCTION

Ultrafast laser pulses are uniquely suited for processing transparent wide band-gap dielectrics.[1] However, a definitive answer to several fundamental questions, including the relative significance of different nonlinear absorption processes, is still lacking. In principle, it is possible to estimate the physical events happening during the process of laser-matter interaction if the detailed behavior of the electrons can be tracked. This is because the laser energy is first absorbed by the electrons, and then transferred to the lattice by electron-phonon coupling. For ultrashort laser pulses, free electrons are initially excited through nonlinear photoionization processes such as multiphoton ionization (MPI) and tunneling photoionization (TPI). In MPI, a single electron can absorb several photons simultaneously to gain enough energy to cross the band gap. On the other hand, at higher values of the electric field, the valence electrons can be injected into the conduction band by Fowler-Nordheim tunneling[2] leading to TPI. The seed electrons excited into the conduction band by the photoionization process continue to absorb laser energy through the inverse bremsstrahlung process. If the kinetic energy of the free electrons exceeds a critical value, the free electrons can ionize other bound electrons in the valence band inducing the avalanche ionization process. A simple rate equation without considering TPI has been derived by Stuart *et al.*[3] to describe the evolution of the free electron density ρ:

$$\frac{d\rho}{dt} = \sigma_n I^n + \beta I \rho, \tag{1}$$

where I is the laser intensity, β the avalanche ionization coefficient, and σ_n the MPI coefficient for n-photon absorption, where n is the smallest integer satisfying $n\,\omega \geq U$. ω and U are the laser frequency and the band gap, respectively. The first term in the equation accounts for MPI and the second term for avalanche ionization.

Many works have been done to study ultrafast laser interaction with transparent materials. The primary approach was to measure the pulsewidth dependence of the optical breakdown threshold (OBT), which was determined differently by various groups. Stuart *et al.*[3,4] defined the OBT as the appearance of visible permanent modification that could be observed under a microscope on a sample surface irradiated by multiple pulses. Lenzner *et al.*[5] obtained the OBT by extrapolating the ablated volume vs laser fluence curve to zero for a sample irradiated with multiple pulses. Du *et al.*[6] defined the OBT as the laser fluence at which a sharp increase in plasma emission and change in the transmitted energy was observed for single pulses. Li *et al.*[7] also measured the OBT by the plasma emission technique. Varel *et al.*[8] used both plasma emission and multiple- and single-shot damage techniques. Since optical breakdown in transparent dielectrics is associated with the rapid buildup of free electrons to a critical density,[9] the MPI and avalanche ionization coefficients can be obtained by fitting Eq. (1) to the measured values of the OBT. However, the different measurement techniques yielded widely different values for these coefficients. For example, the MPI coefficient for fused silica was measured to be $6\times10^{-70}(\mathrm{m^2/W})^6\,\mathrm{s^{-1}\,m^{-3}}$ by Lenzner *et al.*,[5] which is four orders of magnitude higher than the value of $3\times10^{-74}(\mathrm{m^2/W})^6\,\mathrm{s^{-1}\,m^{-3}}$ reported by Li *et al.*[7] The discrepancy can be due to the subjective nature of visual observation of optical damage, the uncertain relation between plasma emission and optical breakdown in the plasma emission technique, and the incubation effect[10] that can decrease the value of the OBT during multiple pulse measurements.

The OBT measurements have also been used to estimate the avalanche ionization process by fitting Eq. (1), e.g., Lenzner *et al.*[5] obtained a value of 4 $\mathrm{cm^2/J}$ for β. This leads to a scenario where photoionization provide the initial free electrons which seed the avalanche process that finally leads to optical breakdown.[6] However, whether avalanche ionization really plays a major role has been doubted by some researchers. Simulation results for fused silica from Arnold *et al.*[11] based on both standard classical approximations and quantum-mechanical theory show that the material can be efficiently heated and melted due to MPI absorption even before avalanche ionization happens. Simulations for fused silica based on the Boltzmann kinetic equation reported by

Kaiser *et al.*[12] also show that the free electrons are generated mainly by nonlinear photoionization and that avalanche ionization is of minor importance for laser pulses shorter than 100 fs. Time-resolved frequency-domain interferometric pump-probe results from Quéré *et al.*[13] also demonstrate that MPI is responsible for the creation of free electrons and no sign of avalanche ionization was observed for pulses shorter than a few ps. Based on the OBT measurements of transparent dielectrics by plasma emission technique for 1 ps laser pulses as a function of mid-IR wavelength from 4.7 to 7.8 μm, Simanovskii *et al.*[14] concluded that seed electrons are generated by TPI with subsequent avalanche ionization for wide-gap dielectrics and TPI alone leads to optical breakdown for narrow-gap dielectrics.

In order to avoid the uncertainty surrounding the OBT measurements, a logical way is to monitor changes in the laser beam itself as the fluence is increased. In this work, both experiments and numerical simulation of single pulse transmissivity are carried out to study how the ultrafast laser pulse is coupled into fused silica. The initial part of the laser pulse creates free electron plasma by the absorption processes discussed previously. This plasma can then absorb and reflect the later part of the pulse. As such, comparison between the calculated and measured transmissivity of a single pulse can provide information about the laser absorption process. Similar measurements of single pulse reflectivity for plasma mirror applications have been reported previously by Doumy *et al.*[15] All the measurements reported in this work have been taken at the single pulsewidth of 90 fs, which is similar to the case of Li *et al.*[7] who conducted their experiment with 25 fs pulses. The other OBT studies reported above varied the pulsewidth widely from about 10 fs to several ps. However, avalanche ionization becomes more important as the pulsewidth is increased. Our work concentrates on studying the relative roles of nonlinear photoionization and avalanche ionization for pulses on the order of 100 fs. In Sec. II below, the simulation model is presented. The experiments and comparison to the experimental results are given in Sec. III, which allows us to evaluate the relative contribution of nonlinear photoionization and avalanche ionization in the free electron generation process.

II. MODEL

Assuming the laser pulse propagates along the z axis, we model the linearly polarized laser by the envelope function $\psi(r,z,t)$ of the electric field $E(r,z,t)=\psi(r,z,t)\exp(ikz-i\omega_0 t)$, where r, k, ω_0 are the cylindrical radial coordinate, the wave number, and the laser center frequency, respectively. The laser intensity $I=nc_0\varepsilon_0|\psi|^2/2$ where n, c_0, ε_0 are the refractive index, the light speed in vacuum, and the vacuum permittivity constant, respectively. The scalar function ψ is assumed to vary slowly in time t and along z. It evolves according to the following 2(spatial)+1(temporal) propagation equation[16] in a reference frame moving at the group velocity v_g

$$\frac{\partial}{\partial z}\psi = \frac{i}{2k}\nabla_t^2\psi - \frac{W_{\mathrm{PI}}U}{nc_0\varepsilon_0|\psi|^2}\psi - i\frac{k''}{2}\frac{\partial^2\psi}{\partial t'^2} + \frac{i}{2k}k_0^2(\varepsilon - n^2)\psi, \tag{2}$$

where ∇_t^2 is the Laplacian operator in the transverse plane, W_{PI} is the photoionization rate, k'' is the group velocity dispersion coefficient, $t'=t-z/v_g$ is the retarded time, k_0 is the laser wave number in vacuum, ε is the complex relative dielectric constant of excited fused silica, and $n=\mathrm{Re}\sqrt{\varepsilon}$ is the corresponding refractive index. The first term on the right-hand side (RHS) in Eq. (2) stands for laser diffraction in the transverse plane, the second term accounts for absorption due to nonlinear photoionization, and the third term represents the group velocity dispersion. The last term of the RHS is discussed as follows.

According to the Drude model,[17] the complex relative dielectric constant of fused silica with free electron density ρ in the conduction band can be written as

$$\varepsilon = \varepsilon^0 - \frac{e^2\tau}{m\omega\varepsilon_0(i+\omega\tau)}\rho, \tag{3}$$

where e, τ, m, ε^0 are the electronic charge, the electron collision time, the effective mass of the free electron, and the relative dielectric constant of fused silica without any free electrons, respectively. The first term on the RHS represents the effect of the bound electrons and the second term accounts for the effect of the free electrons in the conduction band. Considering the optical Kerr-effect, the dielectric constant in Eq. (3) becomes

$$\begin{aligned}\varepsilon &= (n_0 + n_2 I)^2 - \frac{e^2\tau}{m\omega\varepsilon_0(i+\omega\tau)}\rho, \\ &\approx n_0^2 + 2n_0 n_2 I - \frac{e^2\tau}{m\omega\varepsilon_0(i+\omega\tau)}\rho,\end{aligned} \tag{4}$$

where n_0, n_2 are the refractive index in the absence of the laser and the Kerr-effect coefficient, respectively. As an approximation in the case of weak laser intensity, the effect of the free electrons on the wave number is negligible, i.e., $k \approx n_0 k_0$. Substituting Eq. (4) into Eq. (2) yields

$$\begin{aligned}\frac{\partial}{\partial z}\psi = \frac{i}{2k}\nabla_t^2\psi - \frac{W_{\mathrm{PI}}U}{nc_0\varepsilon_0|\psi|^2}\psi - i\frac{k''}{2}\frac{\partial^2\psi}{\partial t'^2} + ik_0 n_2\frac{nc_0\varepsilon_0}{2}|\psi|^2\psi \\ - \frac{\sigma}{2}\rho\psi - i\frac{\sigma}{2}\omega\tau\rho\psi,\end{aligned} \tag{5}$$

where $\sigma=(1/nc_0\varepsilon_0)[e^2\tau/m(\omega^2\tau^2+1)]$ is the cross section of the inverse bremsstrahlung absorption for a single electron. The above Eq. (5) is identical to the laser propagation equation used by Sudrie *et al.*[18] The last three terms on the RHS, which correspond to the last term in Eq. (2), account for self-focusing related to the Kerr effect, free electron absorption, and laser defocusing due to free electrons, respectively.

The photoionization rate W_{PI} is related to the band gap U, electric field angular frequency ω, effective electron mass m, and the electric field E using the Keldysh theory[19]

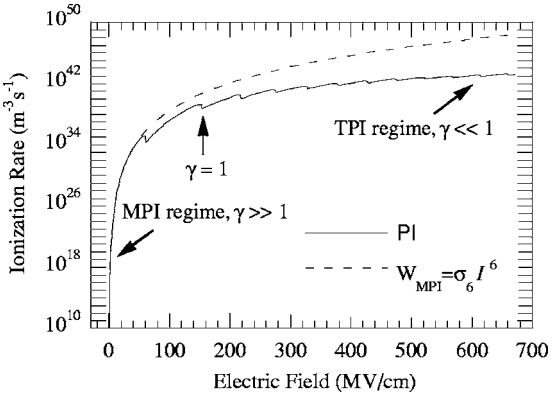

FIG. 1. The electric field dependence of the photoionization rate W_{PI} based on Keldysh's theory for fused silica with band gap 9.0 eV irradiated by 800 nm laser.

$$W_{\mathrm{PI}(\omega,m,U,E)} = \frac{2\omega}{9\pi}\left(\frac{m\omega}{\sqrt{\gamma_1}}\right)^{3/2} Q_{(\gamma,x)} \times \exp\left(-\pi\langle x+1\rangle \frac{K_{(\gamma_1)} - E_{(\gamma_1)}}{E_{(\gamma_2)}}\right), \quad (6)$$

where the Keldysh parameter $\gamma = \omega\sqrt{mU}/eE$, $\gamma_1 = \gamma^2/(1+\gamma^2)$, $\gamma_2 = 1-\gamma_1$, $x = (2/\pi)(U/\omega)(\sqrt{1+\gamma^2}/\gamma)E_{(\gamma_2)}$, and the symbol $\langle x\rangle$ denotes the integer part of x. K and E are the complete elliptic integrals of the first and second kinds. The function

$$Q_{(\gamma,x)} = \sqrt{\frac{\pi}{2\,\mathrm{K}_{(\gamma_2)}}}\sum_{n=0}^{\infty}\left\{\exp\left(-n\pi\frac{\mathrm{K}_{(\gamma_1)} - \mathrm{E}_{(\gamma_1)}}{\mathrm{E}_{(\gamma_2)}}\right) \times \Phi\left(\pi\sqrt{\frac{2\langle x+1\rangle - 2x + n}{2\mathrm{K}_{(\gamma_2)}\mathrm{E}_{(\gamma_2)}}}\right)\right\},$$

where $\Phi(x) = \exp(-x^2)\int_0^x \exp(y^2)dy$ is the Dawson function. Figure 1 shows the electric field dependence of the photoionization rate W_{PI} in fused silica based on the Keldysh theory. The band gap of fused silica is $U = 9.0$ eV,[18] the laser wavelength is 800 nm, and the effective electron mass is 0.86 m_e (Ref. 20) (m_e is the free electron mass). In the case of low frequency and strong field $\gamma \ll 1$, photoionization is achieved mainly by the TPI process. In the opposite limit of $\gamma \gg 1$, MPI is the dominant process. If only MPI is considered in the calculation, an MPI coefficient is fitted to be $\sigma_6 = 5.78\times10^{-66}(\mathrm{m}^2/\mathrm{W})^{-6}\,\mathrm{s}^{-1}\,\mathrm{m}^{-3}$, and the corresponding MPI rate is also shown in Fig. 1 for comparison.

Along with the photoionization rate, the following rate equation can be used to describe the evolution of the free electron density in fused silica:

$$\frac{d\rho}{dt} = (W_{\mathrm{PI}} + \beta I\rho)\left(1 - \frac{\rho}{\rho_{\max}}\right) - \frac{\rho}{\tau_s}. \quad (7)$$

The first term on the RHS is equivalent to Eq. (1) with additional considerations of TPI and the available bound electron density in the valence band with $\rho_{\max} = 2.2\times10^{22}$ cm^{-3}. The second term considers the free electron loss due to electron trapping with a trapping time $\tau_s = 150$ fs,[21] which was neglected in Ref. 3. The avalanche ionization coefficient β is defined as[18]

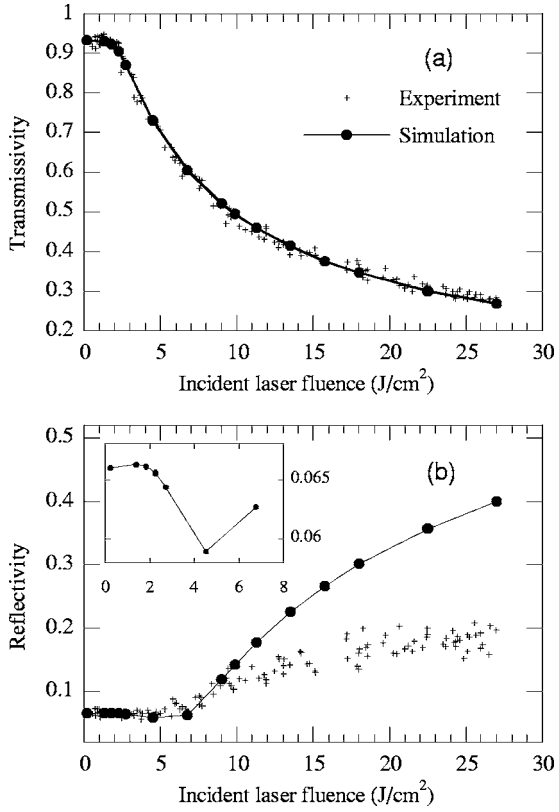

FIG. 2. Laser fluence dependence of single pulse (a) transmissivity and (b) reflectivity of fused silica irradiated by 800 nm, 90 fs laser pulses. The simulation results are also shown for comparison with the experimental data. Inset in (b): simulated reflectivity for laser fluence less than 6.8 J/cm^2.

$$\beta = \sigma/U', \quad (8)$$

where the effective band gap $U' = (2 - m/m_e)(U + e^2E^2/4m\omega^2)$,[12] which takes into account the oscillation energy of the free electrons in the electric field, and the conservation of energy, and momentum during the collision between free and bound electrons.

The laser propagation Eq. (2) is coupled with the rate Eq. (7). In this work, these two equations are solved simultaneously by means of a Crank-Nicholson finite-differencing scheme to obtain the spatial and temporal dependence of the free electron density and the spatial and temporal dependence of laser intensity inside the fused silica. At the air-sample interface, the transmitted and reflected field intensity is calculated by multiplying the incident intensity by the time-dependent transmissivity $[2/(1+\sqrt{\varepsilon_{(t)}})]$ and reflectivity $[(1-\sqrt{\varepsilon_{(t)}})/(1+\sqrt{\varepsilon_{(t)}})]$ determined from Eq. (4).[1,3]

III. RESULTS AND DISCUSSION

A. Experiments

The laser system used in the experiments is a commercial Ti:sapphire ultrafast regenerative amplifier system from

TABLE I. Summary of parameters used in the simulation.

	Symbol	Description	Value
Constants	c_0	Velocity of light in vacuum	3×10^8 m/s
	m_e	Free electron mass	0.91×10^{-30} kg
	ε_0	Vacuum permittivity	8.854×10^{-12} F/m
	e	Electron charge	1.6×10^{-19} C
		Planck's constant	1.06×10^{-34} J/s
Laser properties	λ_0	Laser wavelength in vacuum	800 nm
	w_0	Beam radius in air at the focal point	2.0 μm
	τ_p	Pulsewidth (Intensity FWHM)	90 fs
Sample properties (fused silica)	U	Band gap	9.0 eV (Ref. 18)
	m	Effective mass of electron	0.86 m_e (Ref. 20)
	τ_s	Electron trapping time	150 fs (Ref. 21)
	k''	Group velocity dispersion coefficient	361 fs^2/cm (Ref. 18)
	n_0	Refractive index of fused silica	1.45 (Ref. 18)
	n_2	Self-focusing coefficient	3.54×10^{-16} cm^2/W (Ref. 18)
	τ	Electron collision time	1.0 fs
	$\rho_{\max}$	Maximum electron density	2.2×10^{22} cm^{-3}

Spectra-Physics, which outputs 90 fs FWHM pulses with energy up to 1 mJ/pulse at a center wavelength of 800 nm, and a repetition rate of 1 kHz. A shutter (Uniblitz LS6T2) triggered by the laser was used to admit a single pulse from the pulse train. The sample was moved laterally by 15 μm after each shot to ensure that each measurement is at a fresh spot. The horizontally polarized pulses were then focused normally on the polished fused silica sample (Alfa Aesar, 1 mm thick) with a Mitutoyo long working distance objective (10×, 0.28NA). The beam diameter at the focus was measured to be 4.0 μm by the scanning knife-edge technique. The transmitted beam was collected with a 50× objective (0.5NA), and the reflected beam was collected by the Mitutoyo objective itself. The magnitudes of the incident, transmitted, and reflected beams were measured with silicon PIN detectors (Thorlabs, DET110). Appropriate neutral density filters were used before the detectors to ensure that they operated in the linear regime. Band pass filters and polarizers were added in front of the detectors to ensure that only the desired part of the pulse could reach the detectors. The incident laser energy was adjusted with a half wave plate and polarizer combination. The signals from the detectors were measured with an oscilloscope (Tektronix TDS744).

The sample itself was mounted on a mirror mount with adjustable tilt angles. A CCD imaging system was used to monitor the front surface of the sample during the experiments. It was observed that the transmissivity and reflectivity measurements were quite sensitive to the position of the front surface of the sample relative to the focus. The imaging system helped to ensure that the beam was normal to the sample and that the sample surface stayed in focus during the experiments.

B. Comparison of the simulation to the experimental results

Figure 2 shows the measured single pulse transmissivity and reflectivity as a function of laser fluence. The parameters used in the simulation are listed in Table I. As expected, the transmissivity drops and the reflectivity increases as the incident fluence is increased since the free electron plasma density ρ increases with increasing fluence leading to greater change in the dielectric constant ε as predicted by Eq. (4). The simulation results without considering avalanche ionization in the Eq. (7), i.e., $\beta=0$, are shown for comparison with the experimental data. It is seen that, without considering avalanche ionization, the calculated result for transmissivity is in excellent agreement with the experimental data. The single pulse transmissivity starts to decrease from 0.934 at an incident laser fluence of 2.25 J/cm^2 to 0.280 at 27.0 J/cm^2. For our experimental conditions, 1.0 μJ/pulse corresponds to a fluence of 9.0 J/cm^2 and an intensity of 166 TW/cm^2. Visible damage on the sample surface could be observed by the CCD imaging system when the incident laser energy was about 4 J/cm^2.

The single pulse reflectivity data in Fig. 2(b) shows that it increased from a value of about 0.066 at fluences below $\sim$7 J/cm^2 to about 0.2 at 27.0 J/cm^2. It is seen that the reflectivity data has larger fluctuations compared with the transmissivity data and that the calculated reflectivity exceeds the experimental values by a wide margin when the laser fluence is above 9.0 J/cm^2. This is in contrast to data on the plasma mirror effect that has been reported previously[15] wherein it was shown that good agreement between single-pulse reflectivity data and predictions from a model similar to ours could be achieved. This discrepancy in the reflectivity data in our case is due to a significant amount of nonspecular reflection or scattering in the case of the high incident laser fluences. As the nonspecular light is not collected, the measured reflectivity is less than the total reflectivity. The reason for strong scattering in our experiment is because of the tight focusing conditions that were employed that led to a much more spatially confined and inhomogeneous plasma. In the previous report,[15] the focusing was

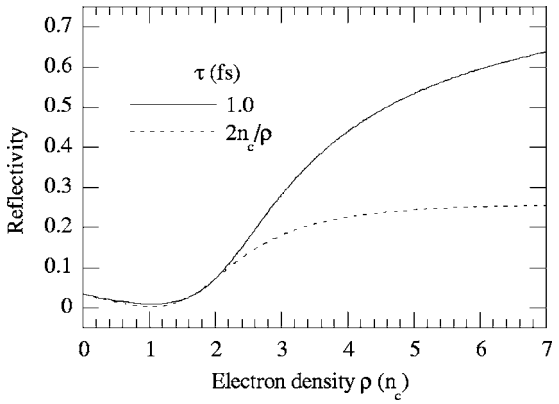

FIG. 3. The free electron density dependence of reflectivity based on Eq. (3) with assumption of constant collision time and variable collision time.

done with a 1200 mm focal length lens which led to a spot size of 30 μm, much larger than our spot size of 4 μm. Moreover, the beam profile was top-hat which led to homogeneous and uniform plasma. Another reason for the discrepancy between the predicted and measured values of reflectivity could arise from the assumption of a constant electron collision time used in the simulation that overestimates the reflectivity. The collision time τ in Eq. (4) will be decreased when the free electron density is increased to near the critical density ($n_c=1.5\times10^{21}$ cm^{-3}), resulting in a decrease of reflectivity. This decrease in the collision time has been reported in the literature and an inversely proportional relation with the free electron density has been suggested.[22] This is illustrated in Fig. 3 where the simulated reflectivity for constant collision time $\tau=1.0$ fs is compared with the case where the collision time varies inversely with free electron density $\tau=2n_c/\rho$ fs. Figure 3 shows that the reflectivity with variable collision time is much less than the reflectivity with a constant collision time when the free electron density is above $2n_c$. As will be shown later, our calculations show that varying the collision time τ does not lead to much variation in the predicted transmissivity. As such, a variable collision time might provide a better fit to our reflectivity data while preserving the transmissivity fit. However, the uncertainty in determining the exact relation between collision time and free electron density and the fact that electron temperature also has an effect on electron collision time[22] led us to choose to use a constant value for our model.

The calculated reflectivity also shows another feature, which can be explained by Eq. (4). As shown in the inset in Fig. 2(b), at lower laser fluences the calculated reflectivity first increases slightly and then decreases until the laser fluence reaches 4.5 J/cm^2. Unfortunately, these changes are too small to be detected in our experiments as they fall within the noise limits. When the laser fluence exceeds 6.75 J/cm^2, the reflectivity increases dramatically. In the case of low laser fluences (<1.4 J/cm^2), the dielectric constant is proportional to the laser intensity as shown in Eq. (4) because of the negligible free electron density, resulting in the slight increase in reflectivity. When the laser fluence is further increased, the effect of the free electrons on the dielectric constant causes a slight decrease of reflectivity. Finally, when

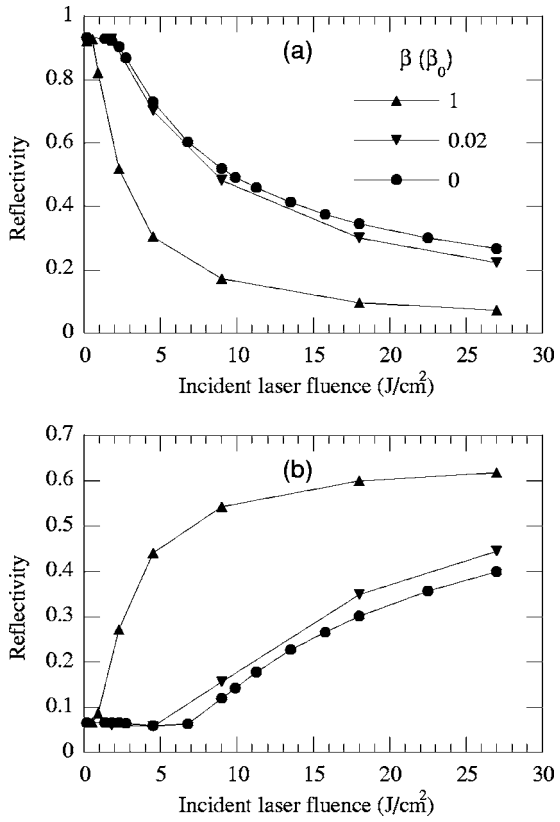

FIG. 4. Simulation results of (a) transmissivity and (b) reflectivity with different values of the avalanche ionization coefficient. The results without avalanche ionization are also included for comparison.

the laser fluence exceeds 6.75 J/cm^2, the rapid increase of the free electron density leads to the drastic increase of reflectivity.

As shown in Fig. 2(a), the calculated transmissivity agrees well with the experimental data when avalanche ionization is not considered, i.e., $\beta=0$ in Eq. (7). If the value of the avalanche ionization coefficient is computed using Eq. (8), it is found to lie between 6.9 to 15.7 cm^2/J depending on the laser fluence. Using the value calculated from Eq. (8), represented as β_0, the corresponding transmissivity are calculated and plotted in Fig. 4. It is seen that the calculated transmissivity deviates greatly from the experimentally measured values which were shown to match closely with the case where $\beta=0$ in Fig. 2(a). To match the calculated results with the experimental data within the experimental uncertainty, the avalanche ionization coefficient should be less than $0.02\beta_0$ (in the range from 0.14 to 0.31 cm^2/J), which is much smaller than the values fitted by Lenzner *et al.*[5] (4.0 cm^2/J), Li *et al.*[7] (9.0 cm^2/J), and Doumy *et al.*[15] (11.0 cm^2/J). This discrepancy can be due to the following two reasons. First, the simple MPI expression ($W_{\mathrm{MPI}}=\sigma_n I^m$) in Eq. (1) is not valid when the corresponding electric field is high ($\sim$236 MV/cm when optical breakdown occurs at about 4 J/cm^2). At this fluence level, the corresponding Keldysh parameter $\gamma\sim0.66$, where the nonlinear photoionization is primarily due to tunneling.[5,9,19] The underestimated MPI coefficients fitted by Lenzner *et al.*[5]

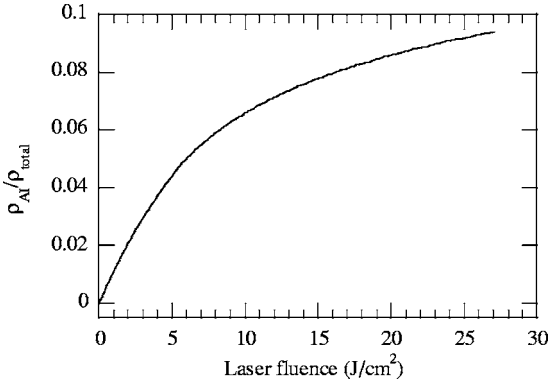

FIG. 5. The ratio of free electrons generated by avalanche ionization to the total free electrons on the sample surface as a function of laser fluence with avalanche ionization coefficient $\beta=0.02\,\beta_0$.

$[6\times10^{-70}(\mathrm{m^2/W})^6\,\mathrm{s^{-1}\,m^{-3}}]$, and Li *et al.*[7] $[3\times10^{-74}(\mathrm{m^2/W})^6\,\mathrm{s^{-1}\,m^{-3}}]$ compared with the value of $\sigma_6=5.78\times10^{-66}(\mathrm{m^2/W})^{-6}\,\mathrm{s^{-1}\,m^{-3}}$ obtained from the Keldysh formula in Eq. (6) leads to an overestimation of the avalanche ionization coefficients. The second reason could arise from the uncertainty related to the OBT measurements as discussed previously.

The smaller values of the avalanche ionization coefficient predicted by comparing our simulation results with the experimental transmissivity data naturally lead to a very small fraction of free electrons generated by the avalanche ionization process. This is illustrated in Fig. 5 which shows the ratio of the free electron density generated by avalanche ionization to the total free electron density at the surface of the sample. It is seen that even at the highest fluence of 27 J/cm^2 with an upper bound of avalanche ionization ($\beta=0.02\,\beta_0$), the contribution of avalanche ionization is less than 10% of the total.

Finally, we present results to evaluate the parameters in the calculation that can affect the model predictions. Figure 6 shows the dependence of the calculated transmissivity on the beam spot size and the sample position. It is seen that the predicted transmissivity is sensitive to the beam radius and the position of the front surface of the sample relative to the focal position. Because of these reasons, the beam spot size was carefully measured with the scanning knife-edge technique and a high resolution CCD imaging system was used to maintain constant z position of the sample surface. Experimental results shown in Fig. 6(b) also indicate that transmissivity changes rapidly near $z=0$, and there is a good agreement between the measured and calculated transmissivity as a function of z.

Figure 6(b) also shows that the transmissivity is almost constant when the laser pulse is focused more than $\sim20\ \mu$m below the surface. This is predicted by our model and is verified by single pulse z-scan measurements which monitor the transmission while scanning the sample along the optical (z) axis. These results suggest that measurements carried out in the bulk are more reliable as they do not suffer from measurement uncertainty that may accompany small positioning errors in focusing the beam on the surface. As such, single pulse transmissivity measurements were carried out at

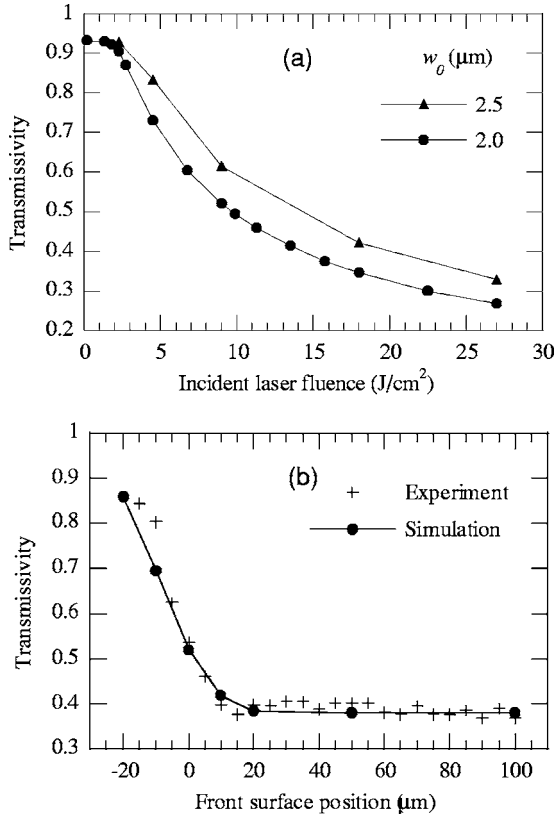

FIG. 6. (a) Beam spot size, and (b) front surface position dependence of transmissivity of fused silica irradiated by 800 nm, 90 fs laser pulses with incident fluence 9.0 J/cm^2. Positive value of position means the beam focal point is inside the sample.

a depth of 75 μm below the surface and the results are shown in Fig. 7. Comparison with model predictions shows that the experimental data agrees well with the model for fluences less than 9 J/cm^2 when avalanche ionization coefficient $\beta<0.02\beta_0$. On the other hand, including avalanche ionization in the model ($\beta=\beta_0$) leads to a rapid decrease in the transmissivity at a lower fluence which does not match the experimental data. This is consistent with the results pre-

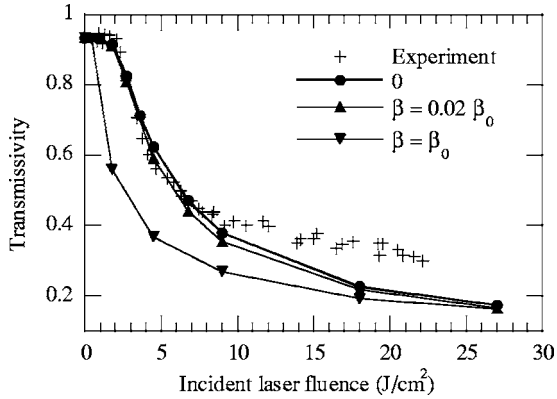

FIG. 7. Laser fluence dependence of single pulse transmissivity of fused silica irradiated by 800 nm, 90 fs laser pulses focused 75 μm below the surface. The simulation results with and without avalanche ionization are also shown for comparison.

sented in Figs. 2(a) and 4(a) for the case where the pulse is focused on the surface.

Figure 7 also shows that the model predictions are below the experimentally observed transmissivity values at higher fluences irrespective of whether avalanche ionization is considered or not. This is partly due to the fact that our model does not provide for scattering from the bulk free electron plasma as has been mentioned before in connection with Fig. 2(b). Computation of scattering from the bulk free electron plasma which gradually changes its density in 3D space is not attempted in this work. However, at lower fluences ($\sim$a few J/cm^2), the scattering (reflectivity) is small as seen in Fig. 2, therefore, a better agreement between the calculation ($\beta=0$) and the experimental data is obtained; while at higher fluences, the reflectivity predictions deviate from the measured values due to stronger scattering from the plasma. Moreover, at the extremely high intensities considered here, the presence of other nonlinear effects in the bulk like white-light generation will affect the transmissivity measurement. Since such effects are not considered in our model, the simulation predictions cannot exactly match the experimental data in the high intensity regime although the general trend in the data is well reproduced.

The effects of the other calculation parameters on the transmissivity predictions were also analyzed. It was seen that the calculated results are quite insensitive to the values of the electron trapping time, effective electron mass, laser pulsewidth, electron collision time, and maximum available electron density. These sensitivity calculations show that single pulse transmissivity measurements can be used to determine the relative importance of nonlinear photoionization and avalanche ionization for free electron generation in fused silica irradiated by ultrafast laser pulses.

IV. CONCLUSION

In summary, experiments and simulations of single pulse transmissivity and reflectivity for fused silica irradiated by 90 fs laser pulses at a center wavelength of 800 nm were performed. The (2+1)-dimensional laser beam propagation equation inside fused silica was numerically solved and the calculated transmissivity values were found to be in excellent agreement with the experimental data. It was also found that the model overpredicted the reflectivity values compared to the experimental data. Comparison between the calculated and the measured transmissivity shows that the avalanche ionization process contributes little to the generation of free electrons inside fused silica, and the observed phenomena is better explained in terms of the nonlinear photoionization mechanisms predicted by the Keldysh formula. The method of monitoring the single pulse transmissivity reported in this work is more accurate and reliable than previous methods that rely on measuring the OBT as the uncertainty surrounding such measurements is removed. Instead the model predictions are fitted to a range of data extending from much below the damage threshold to values that are an order of magnitude higher. This results in much greater confidence in model predictions and evaluation of the different mechanisms involved in free electron generation.

ACKNOWLEDGMENTS

Support for this work by the National Science Foundation and the Indiana 21st Century Research and Development Fund are gratefully acknowledged.

*Author to whom correspondence should be addressed. Electronic address: xxu@ecn.purdue.edu

[1] M. D. Feit, A. M. Komashko, and A. M. Rubenchik, Appl. Phys. A: Mater. Sci. Process. **79**, 1657 (2004), and references therein.
[2] R. H. Fowler, and L. Nordheim, Proc. R. Soc. London, Ser. A **119**, 173 (1928).
[3] B. C. Stuart, M. D. Feit, S. Herman, A. M. Rubenchik, B. W. Shore, and M. D. Perry, Phys. Rev. B **53**, 1749 (1996).
[4] B. C. Stuart, M. D. Feit, A. M. Rubenchik, B. W. Shore, and M. D. Perry, Phys. Rev. Lett. **74**, 2248 (1995).
[5] M. Lenzner, J. Krüger, S. Sartania, Z. Cheng, C. Spielmann, G. Mourou, W. Kautek, and F. Krausz, Phys. Rev. Lett. **80**, 4076 (1998).
[6] D. Du, X. Liu, G. Korn, J. Squier, and G. Mourou, Appl. Phys. Lett. **64**, 3071 (1994).
[7] M. Li, S. Menon, J. P. Nibarger, and G. N. Gibson, Phys. Rev. Lett. **82**, 2394 (1999).
[8] H. Varel, D. Ashkenasi, A. Rosenfeld, R. Herrmann, F. Noack, and E. E. B. Campbell, Appl. Phys. A: Mater. Sci. Process. **62**, 293 (1996).
[9] A.-C. Tien, S. Backus, H. Kapteyn, M. Murnane, and G. Mourou, Phys. Rev. Lett. **82**, 3883 (1999).
[10] M. Lenzner, J. Kruger, W. Kautek, and F. Krausz, Appl. Phys. A: Mater. Sci. Process. **68**, 369 (1999).
[11] D. Arnold, and E. Cartier, Phys. Rev. B **46**, 15 102 (1992).
[12] A. Kaiser, B. Rethfeld, M. Vicanek, and G. Simon, Phys. Rev. B **61**, 11437 (2000).
[13] F. Quéré, S. Guizard, and P. Martin, Europhys. Lett. **56**, 138 (2001).
[14] D. M. Simanovskii, H. A. Schwettman, H. Lee, and A. J. Welch, Phys. Rev. Lett. **91**, 107601 (2003).
[15] G. Doumy, F. Quéré, O. Gobert, M. Perdrix, Ph. Martin, P. Audebert, J. C. Gauthier, J.-P. Geindre, and T. Wittmann, Phys. Rev. E **69**, 026402 (2004).
[16] Q. Wu, M.S. thesis, Purdue University, West Lafayette, 2004.
[17] S. Ramo, J. Whinnery, and T. Duzer, *Fields and Waves in Communication Electronics* (John Wiley & Sons, New York, 1993), p. 684.
[18] L. Sudrie, A. Couairon, M. Franco, B. Lamouroux, B. Prade, S. Tzortzakis, and A. Mysyrowicz, Phys. Rev. Lett. **89**, 186601 (2002).
[19] L. V. Keldysh, Sov. Phys. JETP **20**, 1307 (1965).
[20] S. Zafar, K. A. Conrad, Q. Liu, E. A. Irene, G. Hames, R. Kuehn, and J. J. Wortman, Appl. Phys. Lett. **67**, 1031 (1995)
[21] P. Audebert, Ph. Daguzan, A. Dos Santos, J. C. Gauthier, J. P. Geindre, S. Guizard, G. Hamoniaux, K. Krastev, P. Martin, G. Petite, and A. Antonetti, Phys. Rev. Lett. **73**, 1990 (1994).
[22] C. Quoix, G. Hamoniaux, A. Antonetti, J. C. Gauthier, J. P. Geindre, and P. Audebert, J. Quant. Spectrosc. Radiat. Transf. **65**, 455 (2000).